Contents available at: Sri Lanka Journals Online

Tropical Agricultural Research

Journal Home Page: https://tar.sljol.info

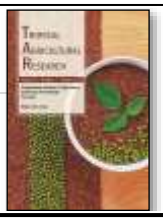

RESEARCH

Two - Stage Catalytic Activation of Coconut Shell Biochar for Effective Malachite Green Removal from Water

T. Bavithira[1,2], N. Kannan[3] and A.K. Karunarathna[4]*

[1]*University College of Jaffna, University of Vocational Technology, Sri Lanka*
[2]*Postgraduate Institute of Agriculture, University of Peradeniya, Sri Lanka*
[3]*Department of Agricultural Engineering, Faculty of Agriculture, University of Jaffna, Sri Lanka*
[4]*Department of Agricultural Engineering, Faculty of Agriculture, University of Peradeniya, Sri Lanka*

ARTICLE INFO

Article history:
Received: 22 March 2024
Revised version received: 20 December 2024
Accepted: 23 December 2024
Available online: 01 January 2025

Keywords:
Adsorption
Engineered biochar
Isotherm
Kinetics
Thermodynamics

Citation:
Bavithira, T., Kannan, N. and Karunarathna, A.K. (2024). Two - Stage Catalytic Activation of Coconut Shell Biochar for Effective Malachite Green Removal from Water. Tropical Agricultural Research, 36(1): 64-81.

DOI:
https://doi.org/10.4038/tar.v36i1.8884

A K Karunarathna
https://orcid.org/0000-0002-9078-400X

*Corresponding author- anujica@agri.pdn.ac.lk

ABSTRACT

This study investigates scientific insights into the adsorption mechanism of novel engineered biochar derived from coconut shells via catalytic conversion with $FeCl_3$ for Malachite Green removal. This is a unique research report describing the use of novel engineered biochar derived from waste coconut shells for the removal of the cationic dye "Malachite Green" by understanding the insights into the adsorptive removal mechanism. The engineered biochar was prepared with different concentrations (5 %, 7 %, and 9 %) of iron catalyst ($FeCl_3$) and at different pyrolysis temperatures: 200 °C, 300 °C, and 400 °C with residence time of 4 hours. An adsorption analysis was planned under the set of experimental conditions: dosage 1g/L; pH 6; rpm 150; holding time 72 hours to identify the best-engineered biochar. The adsorptive performance was checked with artificially polluted water. The engineered biochar with the high q_e value (amount of adsorbate removed by unit weight of engineered biochar) was selected. Detailed isotherm analysis, Kinetics study, thermodynamics analysis, and rate-limiting factor analysis were carried out for engineered biochar with higher adsorptive capacity. The biochar treated with 9% $FeCl_3$ and pyrolysed at 400 °C showed the highest adsorption capacity of 50.20 mg/g for Malachite Green due to increased mineral components and a denser carbon network. Isotherm analysis revealed that the Freundlich model fits well, and the adsorption nature of Malachite Green by 9% CSBC 400 is a multilayer. The results of the adsorption kinetic study revealed that the pseudo-second order model fits well, indicating that the chemisorption process plays a significant role in the removal of Malachite Green by 9% CSBC 400. The adsorption process is spontaneous and endothermic. Therefore, the engineered biochar produced by the iron catalyst is a novel adsorbent for Malachite Green removal. This innovative finding of the use of engineered biochar produced from coconut shells for the removal of malachite green opens the door to the development of novel strategies for the effective removal of dye at the commercial level.

INTRODUCTION

Presently, there are over 0.1 million synthetic dyes in existence, with annual generation exceeding 7.9 million tonnes (Mittal et al., 2009; Raval et al., 2017). When the dyes are discharged into the natural water bodies lead to acute and chronic effects on the organisms, reducing light penetration, restricting oxygen solubility, reducing water transparency and reducing the photosynthetic activity of aquatic plants (Imran et al., 2021). Removing these colourants from industrial wastewater is vital due to their toxicity, even at lower concentrations. As a consequence of their stable chromophore groups, they showed resistance to light, aerobic digestion, and oxidising agents (Alipour et al., 2021). Malachite Green dye usage is widespread throughout several industries, including agriculture, food, and textiles, for various application (Tewari et al., 2018). This dye is a non-azo dye generally utilised for dyeing silk, wood, nylon and cotton in the textile industries and in paper and leather industries (Geetha et al., 2015).

It exhibits suitability as a colouring agent across different industries because of the application span of the Malachite Green dye. Malachite green is a common micro-pollutant in industrial effluent, causing a threat to green flora (Sharma et al., 2023). Previously, Malachite Green was extensively used in the fish farming industry due to its cost efficiency and effectiveness in battling external fungal and parasitic infections in fish (Li et al., 2008; Pan and Zhang, 2009). According to previous studies, Malachite Green is highly hazardous and consequently poses a significant risk to human health. It is a non-biodegradable dye, so it persists in the environment and gets into the food chain, causing genotoxic, mutagenic, and carcinogenic effects (Sharma et al., 2023; Tewari et al., 2018). Hence, restrictions for Malachite Green usage were generated. (Tewari et al., 2018).

Global communities are increasingly advocating for efficient wastewater treatment technologies that minimise harm to ecosystems. Microorganisms and plants are now recognised as effective scavengers for Malachite Green (Sharma et al., 2023). There are several techniques used to remove Malachite Green dye from wastewater. The Malachite Green dye can be removed by coagulation-flocculation (Oladoja and Aliu, 2009), oxidation/advanced oxidation, precipitation, combined chemical and biochemical processes, ozonation(Zhou et al., 2013), aerobic and anaerobic digestion, irradiation, adsorption, membrane treatment (Raval et al., 2022) photocatalytic degradation (Saha et al., 2012), sonochemical catalytic degradation (Moumeni and Hamdaoui, 2012), photooxidative degradation(Modirshahla and Behnajady, 2006), solvent extraction(Pandit and Basu, 2004), solar degradation(Pirsaheb et al., 2016) and adsorption.

Chemical approaches are less advantageous than adsorption technology in terms of operating cost, sustainability, simplicity, resource availability, and operational knowledge (Oladoye et al., 2023). Within the removal techniques of Malachite Green, the adsorption technique effectively eliminates dyes from the liquid phase as it is cheap, fast, and simple (Sangeetha piriya et al., 2021; Tewari et al., 2018).Adsorbents like activated carbons, low-cost materials, nanomaterials (nanotubes, nanofibers, nanorods, and nanowires), composites (chitosan and polyvinyl alcohol) and nanocomposites are used for the adsorption and removal of Malachite Green from wastewater. It has been found that agricultural solid wastes and biosorbents are extensively used among various adsorbents and are considered effective and economical for removing Malachite Green dye (Raval et al., 2017). However, there are still significant knowledge gaps in producing engineered biochar with enhanced functional properties using catalysts, requiring further detailed investigations.

Although many studies have revealed that adding an iron catalyst to biochar improves its surface properties, there is limited understanding of the isotherm, kinetics, and thermodynamics of the adsorption process for Malachite Green removal from aqueous solutions. Since the latter products are more expensive to produce, this study concentrated on the utilization of engineered biochar for dye removal rather than biochar

and activated carbon. The study assessed the potential of engineered biochar prepared from coconut shells for the removal of Malachite Green, which is commonly present in the water bodies which are discharged by industries. Furthermore, the influence of the surface functional properties of the engineered biochar on the adsorption process and the assessment of detailed kinetics, isotherm, and thermodynamic parameters were undertaken to understand the adsorption mechanism of the removal process in order to create new knowledge on biochar.

METHODOLOGY

Materials

Coconut shells were obtained from households in Jaffna, Sri Lanka. The Malachite Green oxalate (Molecular formula: C_{52} H_{54} N_4 O_{12}; Absorption Maxima: 618 nm; dye content: 90.45 %) was used for the experiments.

Sample preparation

The coconut shell was manually chopped with a steel hammer. The resulting particles were sieved through a 2 mm and 1 mm aperture size sieve. The homogenised coconut shells with particle sizes ranging from 1 mm to 2 mm were collected and washed with distilled water. Coconut shell biomass was soaked in 0.5 M HCl for 1 hour to remove acid-soluble organic and inorganic impurities. Afterwards, it was washed again with distilled water and oven-dried at 105 °C for 24 hours.

Preparation of stock solution

Malachite Green stock solution was obtained by dissolving 1 g of exactly weighed Malachite Green Oxalate powder into 1 L of distilled water. The standard calibration curve was obtained for varying concentrations of diluted dye by UV vis Spectrophotometer (Model: UH5300 spectrophotometer) at 618 nm (Abate et al., 2020) against distilled water as a blank.

Impregnation of biomass

The prepared biomass was impregnated with iron chloride hexahydrate ($FeCl_3.6H_2O$) with 99.9% purity. The catalyst was prepared at different concentrations, such as 5, 7, and 9 %. The biomass was mixed using an impregnation ratio (W/V) 1:2 (biomass: Catalyst) with 5, 7, and 9 % concentrations of catalyst (Sunthar et al., 2023). This impregnation ratio was selected based on past research literature as a lower solid: liquid ratio results in wastewater disposal problems (Nadarajah et al., 2021). Then, samples were placed in the mechanical shaker (Rotary shaker NX -25D) operated at 150 rpm at 27 ℃ for 72 hours. Then, samples were drained entirely, filtered with filter paper, and allowed for complete drying by oven drying at 105 °C for 24 hours. The obtained impregnated biomass was labelled as 5 % CS, 7% CS and 9% CS, respectively. (CS: coconut shell; 5 %: catalyst concentration percentage).

Preparation of Coconut shell biochar

Accurately measured 20 g of impregnated and non-impregnated biomass samples were pyrolysed at 200, 300, and 400 °C, respectively, using a muffle furnace (Model: Protherm furnace, PC442T) with a heating rate of 52.8 ℃min^{-1} for 04 hours. The obtained biochar and engineered biochar were labelled as CSBC 200, CSBC 300, CSBC 400, 5% CSBC 200, 5% CSBC 300, 5% CSBC 400, 7% CSBC 200, 7% CSBC 300, 7% CSBC 400, 9% CSBC 200, 9% CSBC 300, 9% CSBC 400. (CSBC: Coconut shell biochar; 5%: Catalyst concentration percentage; 200: Pyrolysis temperature).

Biochar Characterization

The biochar yield was determined using the following equation (equation 01). (Manoharan et al., 2022):

$$\text{Yield} = \frac{\text{Weight of biochar (g)}}{\text{Weight of biomass (g)}} \times 100 \quad \text{.....Equation 01}$$

After that, engineered biochar was soaked in 0.5 M HCl for 1 hour to remove chemical residues. It was again washed with distilled water. Then, samples were drained entirely, filtered with filter paper, and allowed to complete oven drying.

Proximate Analysis

Moisture, volatile matter, and ash content were determined according to ASTM standards (ASTM (2017) – D1762-84). In brief, biochar samples of 1 g in duplicate were heated in crucibles, and the sample weight differences before and after heating were determined. For moisture content, samples were dried at 105 °C for 2 h (oven dry); for volatile matter, samples were heated to 950 °C for 11 min (covered crucible); and for ash content, 750 °C for a minimum of 2 h (uncovered crucible). The weight of the original sample, subtracted by its moisture content, ash content, and volatile matter content, corresponds to the stable carbon fraction of that sample, and hence, this fraction is termed 'fixed carbon or fixed-C fraction' (Ronsse et al., 2013).

Surface charge analysis

The point zero charges of engineered biochar were determined by the pH drift method (Manoharan et al., 2022). The pH of the NaCl solution was adjusted to be in the range of 2 to 10 using 0.1 M HCl solution and 0.1 M NaOH solution. Accurately weighed 0.2 g of biochar pyrolysed at different temperatures was added with 20 mL of NaCl solution with different pH values(Jeganathan et al., 2024). Prepared solutions were placed into the mechanical shaker (Rotary shaker NX -25D) operated at 150 rpm at 27 ℃for 72 hours. The final pH was determined after 24 hours using a pH meter (Model: HM-42X). The pzc value of engineered biochar was determined by the point where the final pH and initial pH values were equal (Manoharan et al., 2022).

Adsorption experiment

Accurately measured 10 mL of 1 g/L Malachite Green standard solution was transferred into 100 mL volumetric flask and volume up to 100 mL by addition of distilled water to obtain 100 mg/L solution. The pH of 100 mg/L solutions was adjusted to 6 using 0.5 M HCl and 0.1 M NaOH. Accurately measured 20 mg of engineered and non-impregnated coconut shell biochar pyrolysed at 200, 300, and 400 °C were added to the flat-bottom glass bottles. Accurately measured 20 mL of 100 mg/L with a pH 6 solution was added to the flat-bottom glass bottles. Three replicates were used for each experiment. Flat-bottom glass bottles with samples were placed into a mechanical shaker (Rotary shaker NX -25D) operated at 150 rpm at 27 ℃for 72 hours.

Distilled water was used as the blank solution. 20 mg of coconut shell biochar pyrolyzed at different temperatures were placed into separate flat-bottom glass bottles. A precise volume of 20 mL of distilled water was poured carefully into glass bottles. A blank setup was also placed into a mechanical shaker with the same conditions as the above sample. After 72 hours, sample bottles were taken out and allowed to settle down. Then, the absorbance of the solution with appropriate dilution was measured using a UV-vis spectrophotometer (UH5300 Spectrophotometer, HITACHI, Japan). Biochar (engineered biochar) exhibited high adsorptive capacity and was selected for further experiments. Malachite Green removal percentage and adsorptive ability were measured using the following equations: 02 and 03.(Manoharan et al., 2022).

$$\text{Removal } \% = \frac{(C_i - C_f)}{C_i} \times 100 \quad \text{.....Equation 02}$$

$$q_e = \frac{V(C_i - C_f)}{W} \quad \text{.....Equation 03}$$

Where Y is the absorbance readings against the blank; q_e is the amount of adsorbate removed per g of adsorbent (adsorption capacity in mg/g); C_i is the initial adsorbate concentration (mg/L); C_t is the adsorbate concentration (mg/L) in solution at time t (h); W is the biochar weight (g); and V is the solution volume (L).

Determination of the influence of the effect of Malachite Green initial concentration, adsorbent dosage and initial pH of solution on the removal of Malachite Green

The effect of engineered biochar dosage on Malachite Green removal was carried out at a temperature of 27 °C with an initial concentration of dye 100 mg/L at pH 6, and the dosage of engineered biochar was set to range 0.5-5 g/L (Sunthar et al., 2023). The effect of pH on Malachite Green removal was

assessed using the initial dosage of 1 g/L with pH ranging from 2 to 10 at 27 °C, and the influence of Malachite Green initial concentration was studied using 1g/L initial dosage with initial concentration ranging from 50 to 300 mg/L at pH 6 (Sunthar et al., 2023).

Adsorption isotherm

Adsorption isotherm studies were carried out using Langmuir, Freundlich, and Temkin models. These studies were carried out to identify whether adsorption is monolayer or multilayer. In nature, the following linear model equations, such as Langmuir (Equation 04), Freundlich (Equation 05), and Temkin (Equation 06), were used for the adsorption isotherm study (Manoharan et al., 2022).

$$\frac{C_e}{Q_e} = \frac{1}{Q_m K_L} + \frac{C_e}{Q_m} \quad \text{.....Equation 04}$$

$$\log q_e = \log K_F + \frac{1}{n} \log C_e \quad \text{.....Equation 05}$$

$$q_e = \frac{RT}{bt} \ln A_t + \left(\frac{RT}{b_t}\right) \ln C_e \quad \text{.....Equation 06}$$

Where q_e is adsorption capacity by weight at equilibrium (mg/g); K_L is the equilibrium constant of adsorption reaction; Ce is the concentration of adsorbate at equilibrium (mg/L); K_L and Qm are Langmuir constant; K_F and n are Freundlich constants; α is initial adsorption rate (mg/g/min); β is Elovich constant (g/mg). The constant values and unknown values were obtained from the slope and intercept of plotted graphs.

Adsorptive kinetics

Malachite green with different initial concentrations of 50, 100 and 150 mg/L was prepared from a stock solution of 1 g/L. The pH of the solution was adjusted to 6 using 0.1 M HCl and 0.1M NaOH. 880 mg of 9 % CSBC 400 was accurately weighed and added into labelled flat-bottom glass bottles separately. Accurately measured 880 mL of Malachite Green solution with different initial concentrations, and pH 6 was added to the glass bottles separately. Two replicates were used for each experiment.

Finally, bottles with samples were placed into a mechanical shaker (Rotary shaker NX -25D) operated at 150 rpm at 27 °C for 72 hours. Distilled water was used as blank and added with 1080 mg engineered biochar separately. Accurately measured 1 mL of solution was taken out at different time intervals: 5, 10, 15, 30, 60, 90, 150, 210, 330, 450, 570, 1290, 1410, 1530, 1650, 1770, 1890, 2010, 2730, 2850, 2970, 3090, 3210, 3330, 3450, 4170, 4290 and 4410 minutes. The volume of the removed solution was 5% of the total volume. Then, the absorbance of the solution with appropriate dilution was measured by UV-vis spectrophotometer (UH5300 Spectrophotometer, HITACHI, Japan).

For adsorptive kinetics, three different models were used to investigate the effect of adsorption rate and find the effect of equilibrium concentration in the adsorptive process (Nadarajah et al., 2021). The models used were the Pseudo-first order kinetics (Equation 07), the Pseudo-second order kinetics (Equation 08), and Elovich (Equation 09) (Manoharan et al., 2022).

$$\log(q_e - q_t) = \log q_e - K_1 \frac{2.303}{} t \quad \text{..... Equation 07}$$

$$\frac{t}{q_t} = \frac{1}{K_2 q_e^2} + \frac{1}{q_e} t \quad \text{..... Equation 08}$$

$$q_t = \frac{1}{\beta} \ln(\alpha\beta) + \frac{1}{\beta} \ln t \quad \text{.....Equation 09}$$

Where the q_e is the amount of adsorbate adsorbed on the adsorbent at equilibrium (mg/g); q_t is the amount of adsorbate adsorbed on the adsorbent at any time t (mg/g), K_1 is the rate constant of the Pseudo-first order adsorption (min^{-1}); K_2 is the rate constant of Pseudo-second order adsorption; α is initial adsorption rate (mg/g/min); β is Elovich constant (g/mg).

Thermodynamics and Rate Limiting Factor Analysis

Thermodynamics analysis was carried out at different temperatures of 27, 33, and 37 °C. The rate equation (Equation 10) and the Van't

Hoff equation (equation 11) can be used for this analysis (Sunthar et al., 2023).

$\Delta G^{\circ} = -RT \ln K_c$ .....Equation 10

Where R is the ideal gas constant [8.314J/ (mole K)]; T is adsorption temperature (K); K_c is the ratio of the equilibrium concentration of the dye ions on the adsorbent to the equilibrium concentration of the dye ions in the solution; and ΔG° is standard free energy

$$\ln K_c = \frac{\Delta H}{R}\frac{1}{T} + \frac{\Delta S^{\circ}}{R}$$ .....Equation 11

Where K_C is the ratio of the equilibrium concentration of the dye ions on adsorbent to the equilibrium concentration of the dye ions in solution; R is the Ideal gas constant (8.314 J/ (mol K)); and T is the adsorption temperature in Kelvin.

The Weber-Morris equation (Equation 12) was used for rate-limiting analysis (Campos et al., 2018).

$q_t = k_{dif} t^{1/2} + C$ ..... Equation 12

Where k_{dif} is intraparticle diffusion constant (g g^{-1} $min^{1/2}$); and C is diffusion resistance constant (g g^{-1})

RESULTS AND DISCUSSION

Biochar characterization

Effect of temperature on non-catalysed biochar yield

Figure 1 illustrates how altering pyrolysis temperature impacts coconut shell biochar yield. The yield of biochar from raw coconut shells declines notably from 90.38 % to 9.89 % as temperature rises. At 200, 300, and 400 °C, the biochar yield is 90.38 %, 29.16 %, and 9.89 %, respectively (Tomczyk et al., 2020). Below the pyrolysis temperature of 200 °C evaporation of moisture and light volatile will take place, and between 200-500 °C devolatilization and decomposition of cellulose and hemicellulose will occur (Tomczyk et al., 2020). Hence, A significant drop, from 90.38 % to 29.16 %, occurs between the temperatures of 200 and 300 °C. Moreover, the biochar yield is significantly affected by the particle size, heating rate, raw material composition, and temperature (Ahmad et al., 2014). Since the raw material, particle size and heating rate are consistent across all biochar, the pyrolysis temperature is the primary factor influencing the yield. Further, pyrolysis temperature crucially impacts the chemical phases and physical states of biochar (Jeganathan et al., 2024; Tomczyk et al., 2020).

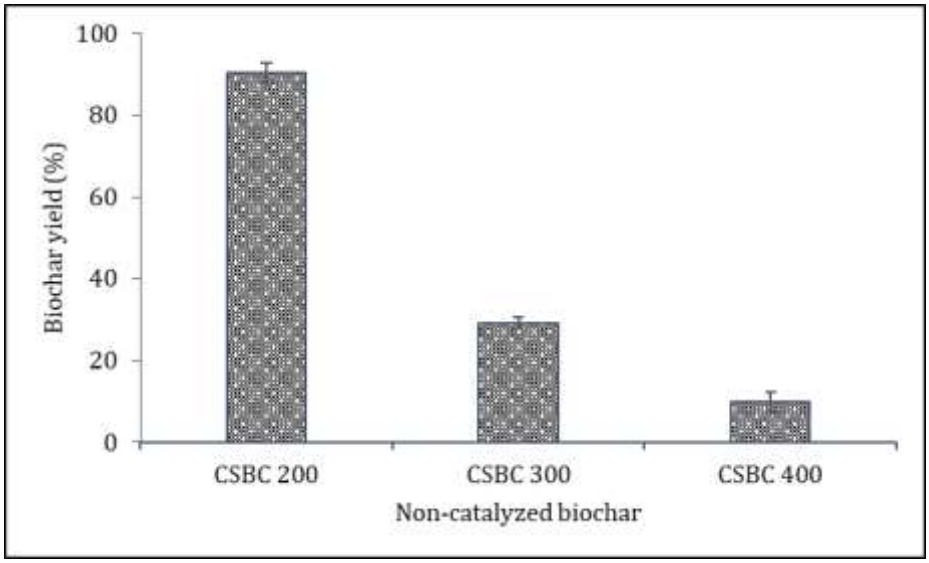

Figure 1. Yield performance of biochar at different pyrolysis temperatures (200, 300, and 400 °C) (Holding time: 4 hrs. and the heating rate at 59.52 ° C/min)

Yield performance of engineered biochar

Activation temperature, impregnation ratio, and $FeCl_3$ concentration are considered important for determining the properties of engineered biochar. As activation temperature and impregnation ratio are maintained as constant, the concentration of $FeCl_3$ has a significant effect on yield determination. The yield of engineered biochar with different $FeCl_3$ concentrations is given in Table 1. Yield of engineered biochar increases with increasing $FeCl_3$ concentration. The yield of engineered biochar increased from 30.27 % to 36.69 % for CSBC 300, and it is from 10.84 % to 13.83 % for CSBC 400 with an increase in $FeCl_3$ concentration from 5 % to 9 %. The chlorine component of the $FeCl_3$ solution catalyses the breakdown of lignin, cellulose, and hemicellulose, allowing for the easier release of tiny molecular hydrocarbons (Li et al., 2016). Furthermore, the dispersed iron species act as in situ catalysts, promoting the small molecules' deposition onto the biochar and increasing the yield of the engineered biochar (Li et al., 2016). Hence, the yield of engineered biochar increased with increasing concentration of iron catalyst at constant pyrolysis temperature.

On the other hand, a reduction in the yield of engineered biochar with the same concentration of catalyst for different pyrolysis temperatures was also observed. This is because of the influence of pyrolysis temperature on biochar yield. In the activation process, the catalyst prompted the creation of certain volatile substances, which were subsequently eliminated through temperature treatment. Therefore, lower yields were observed for engineered biochar than biochar produced without an iron catalyst (Cha et al., 2016).

Proximate analysis

Proximate analysis was performed to measure the moisture, volatile matter, fixed carbon, and ash contained within the produced engineered biochar and raw coconut shell. The moisture contents of the input materials were 10.99 and 6.08 wt % for RCS (Raw Coconut shell) and 9% CSBC 400**,** respectively. It can be visualized from the results that the amount of volatile matter in raw coconut chip**s** was 70.1 % and 24.58 % for 9% CSBC 400. The decrease in volatile matter for 9% CSBC 400 was due to the release of heteroatoms such as oxygen, nitrogen, hydrogen, and sulfur as volatile gaseous products(Sangeetha piriya et al., 2021)The ash content of the RCS was 3.3 %, while it was lower for 9% CSBC 400 (1.59 %). The fixed carbon content of the RCS was 15.61 %, while it increased for 9% CSBC 400 (67.75 %), thus marking its suitability as an adsorbent material.

Surface charge distribution

The point zero charge(pzc) analysis of the engineered biochar was estimated using the pH drift method (Manoharan et al., 2022). The pzc is an important measurement for characterising some materials that are utilized in the environment to treat organic or inorganic wastes, especially wastewater and industrial sludge (Dagnaw and Cherie, 2021). Figure 2 shows the pzc of engineered biochar pyrolyzed at different temperatures (200, 300, and 400 ˚C) with constant concentration of $FeCl_3$. The point at which net anionic and net cationic sites are equal is known as the point zero charge, and it provides a basic description of a material's surface (Dagnaw and Cherie, 2021).

Different pzc values were observed for engineered biochar pyrolyzed at different temperatures. A rise in pzc value was observed with an increase in pyrolysis temperature. The pzc values for 9% CSBC 200, 9% CSBC 300, and 9% CSBC 400 are 2.1, 2.6, and 4.2, respectively. The pzc values increased with pyrolysis temperature as a result of an increase in positively charged ions on the surface of the engineered biochar (Manoharan et al., 2022). The pzc analysis included NaOH, NaCl and HCl for the experimental setup. Accordingly, Cl^- and OH^- compete for positively charged surface sites on the adsorbent, whereas Na+ and H+ compete for negatively charged surface sites (Manoharan et al., 2022). The point at which net positive and negative charges are equal is known as the point zero charge (Jeganathan et al., 2024; Nadarajah et al., 2021).

Table 1. Yield performance of engineered biochar

Pyrolysis temperature (°C)	Catalyst concentration		
	5%	7%	9%
200	87.19	88.62	89.3
300	30.27	31.91	39.69
400	10.84	12.04	13.83

Impregnation ratio(W/V) 1:2 (Biomass: Catalyst)

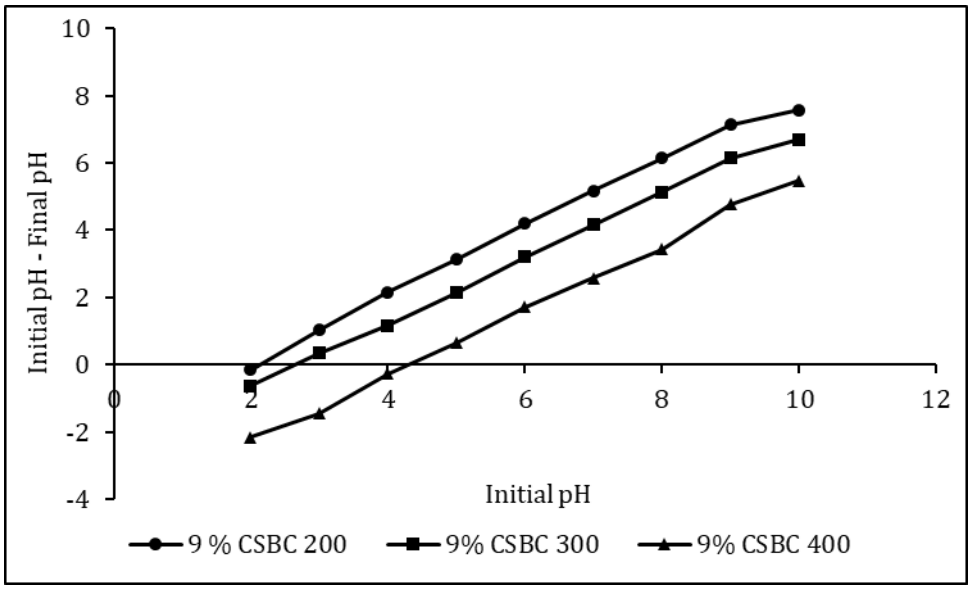

Figure 2. Point zero charge analysis of biochar pyrolysed at different temperatures.

The surface of the biochar will be positively charged below this identified pzc value, and the surface can adsorb anions. It is vice versa for the highest pH values. Therefore, adsorb cations strongly above the pzc value (Farooq and Ramli, 2011; Nadarajah et al., 2021). The best and optimum pH for Malachite Green adsorption can be determined by pzc analysis. (Farooq and Ramli, 2011).

Adsorptive performance of biochar samples

Figure 3 explains the results of the adsorptive performance of coconut shell biochar impregnated and pyrolysed at different temperatures ($FeCl_3$ percentages: Coconut shell biochar: Pyrolysis temperature) 5% CSBC 200, 5% CSBC 300, 5% CSBC 400, 7% CSBC 200, 7% CSBC 300, 7% CSBC 400, 9% CSBC 200, 9% CSBC 300, 9% CSBC 400, CSBC 200, CSBC 300, and CSBC 400). Engineered biochar exhibits mixed adsorptive performance, as shown in Figure 4, due to the variations in surface functional properties like constricted carbon structure and functional groups. The Q_e (amount of adsorbate removed by the unit weight of adsorbent) of 5% CSBC 200, 5% CSBC 300, 5% CSBC 400, 7% CSBC 200, 7% CSBC 300, 7% CSBC 400, 9% CSBC 200, 9% CSBC 300, 9% CSBC 400, CSBC 200, CSBC 300, and CSBC 400 are 19.56, 23.38, 35.62, 27.60, 31.10, 41.66, 31.14, 33.21, 50.22, 10.77, 11.74, and 30.60 mg/g respectively.

The adsorption capacity (Qe) increases as the pyrolysis temperature increases from 200 °C to 400 °C for all $FeCl_3$-impregnated and pyrolysed biochar. This suggests that higher pyrolysis temperatures promote better adsorption capacity of the biochar. According to previous literature, the pyrolysis temperature showed a linear relationship with the surface area and the development of

the constricted carbon structure. The pyrolysis process induces the thermal breakdown of organic materials and the development of channel structure, which leads to an increase in pore volume and surface area (Chatterjee et al., 2020; Manoharan et al., 2022). Furthermore, at each pyrolysis temperature, the adsorption capacity (Qe) rises as the concentration of iron catalyst increases from 5% to 9%. This demonstrates how crucial $FeCl_3$ is in promoting the adsorption performance of the biochar since even the biochar treated with 5% $FeCl_3$ performs better than the CS (noncatalyzed biochar). Based on the previous study chloride has the ability to both improve a biochar's specific surface area and stimulate the thermal breakdown of biomass. Iron is a known catalyst for the successful deposit of small molecular hydrocarbons from biomass pyrolysis, including CH_4, C_2H_4, and C_2H_2 (Li et al., 2016).Hence, The FeCl3 act as a catalyst and it induces the rate of adsorptive performance by enriching the oxygen-containing surface functional groups(Nadarajah et al., 2021).

Additionally, to assess the efficacy of engineering biochar, the adsorptive performance of raw coconut shell (RCS), coconut shell biochar (CSBC 400), and coconut shell-derived engineered biochar (9% CSBC 400) were compared. The obtained results are displayed in Figure 4. An increase in adsorptive performance was observed from raw coconut shell to engineered biochar derived from coconut shell. It results from the activation of surface functional groups and the distribution of pores on the surface (Sunthar et al., 2023). The previous study, "Insights into mechanisms of novel engineered biochar derived from neem chips via iron catalyst for the removal of methyl orange from aqueous phase", reported a similar pattern (Sunthar et al., 2023).

According to the results, the Qe value (mg/g) for 9% CSBC 400 exhibited a higher value of 50.20 mg/g. In addition, CSBC 200 expressed the lowest adsorptive performance compared to other biochar. Hence, engineered biochar impregnated in 9 % $FeCl_3$ and pyrolyzed at 400 ˚C exhibited excellent adsorptive performance in terms of mg/g and removal percentage, indicating that this combination of pyrolysis temperature and iron catalyst concentration is most effective for enhancing engineered biochar adsorption capacity (Qe). The engineered biochar 9% CSBC 400 was selected as the best biochar based on adsorptive performance on Malachite green removal and used for further experiments (isotherm, kinetic and thermodynamics).

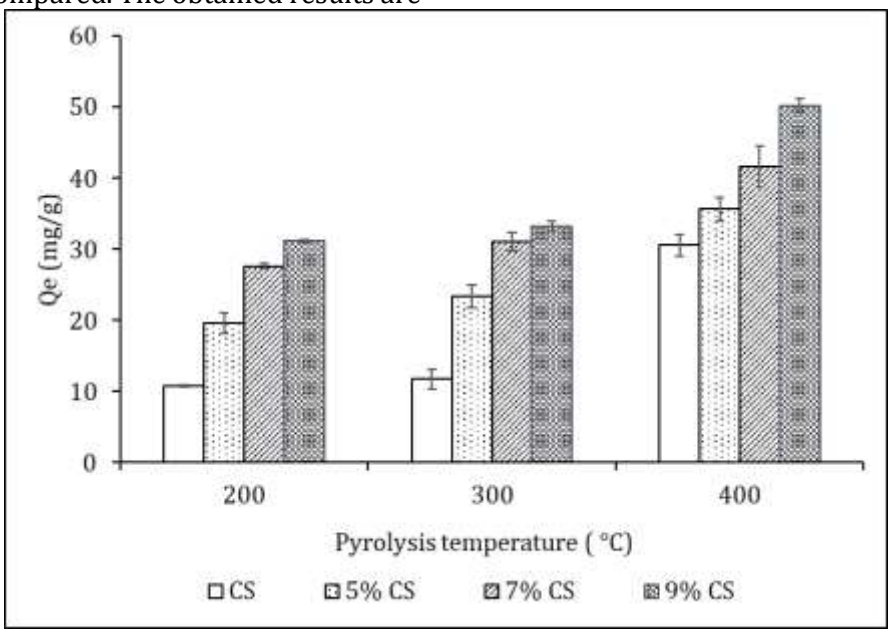

Figure 3. Adsorptive performance of engineered biochar pyrolysed at different temperatures and different $FeCl_3$ concentrations.

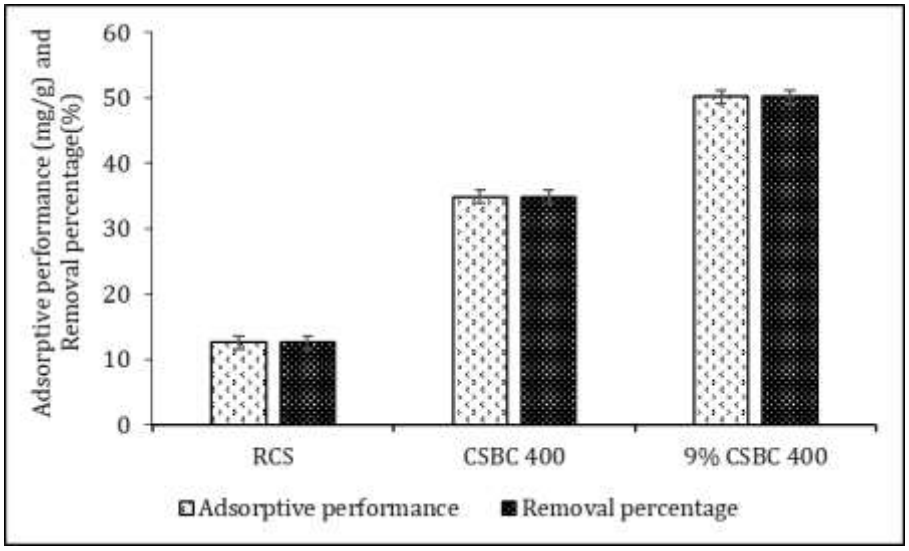

Figure 4. Adsorptive performance and removal percentage of raw coconut shell, biochar (noncatalyzed), and engineered biochar (Temperature: 27 ˚C, pH:6, Dosage 1g/L, Concentration: 100 mg/L)

Dosage

Figure 5 shows changes in the adsorptive performance of 9 % CSBC 400 with different biochar dosages. The adsorptive performance Qe (mg/L) of 9% CSBC 400 for Malachite Green, was dropped with increasing adsorbent dosage. The Qe values of 9% CSBC 400 at adsorptive dosages of 0.5 g/L, 1 g/L, 2 g/L, 3 g/L and 5 g/L are 48.92, 50.20, 34.11, 32.28 and 19.87 mg/g respectively. As dosage increases, there is the possibility of having increased active surface sites on the engineered biochar (Manoharan et al., 2022). However, the adsorptive performance is reduced due to the limited availability of Malachite Green molecules in the adsorptive system (Manoharan et al., 2022).

The removal performance of 9% CSBC 400 for Malachite Green in the percentage varies from the above scenario as it refers solely to the initial concentration (Manoharan et al., 2022). The removal percentage of 9% CSBC 400 at adsorptive dosages of 0.5 g/L, 1 g/L, 2 g/L, 3 g/L and 5 g/L are 24.26, 50.19, 68.22, 96.84 and 99.35 % respectively. As the dosage of the adsorbent increases, there is a potential for increased removal performance attributed to hydrophobic interaction. Hence, an optimal dosage of 9% CSBC 400 at 5 g/L could be selected for effectively removing Malachite Green, considering this aspect. Furthermore, the higher adsorptive performance of Malachite green resulted from the availability of a higher mass of 9% CSBC 400. This higher mass facilitated the formation of an effective, attractive force, significantly enhancing the adsorption process (Nadarajah et al., 2021). In addition, higher biochar dosage exhibits higher adsorption surface area and an increase in the adsorption sides (Jia et al., 2018). Thus, the removal efficiency of 99.41 % was obtained for the engineered biochar dosage of 5 g/L.

Initial Concentration

Figure 6 describes the effect of the initial concentration of Malachite Green on the adsorptive performance of 9% CSBC 400 at 27 °C with a dosage of 1 g/L and pH at 6. The Qe values of 9% CSBC 400 at a dosage of 1 g/L, temperature at 27 °C and pH of 6 with the initial concentrations of 50, 100, 150, 200, and 300 mg/L are 16.51, 43.31, 69.09, 111.48, and 198.59 mg/g respectively. The adsorptive performances in terms of Qe (mg/g) increase with an increase in the initial concentration of Malachite Green. On the other hand, the reduction in removal percentage was observed with increasing initial dye concentration. Removal percentages for initial concentrations of 50, 100, 150, 200 and 300

mg/L are 50.59, 50.19, 45.02, 42.70 and 43.51 %, respectively. As a constant dosage of 9% CSBC 400 has been used, the availability of active sites on the engineered biochar has been considered to be a limiting factor (Pal et al., 2013). Accordingly, the ratio between the active sites on the engineered biochar and dye particles is high for lower initial concentrations of dye. Hence, a high removal percentage was observed for lower initial concentrations of dye(Garg et al., 2003; Sunthar et al., 2023).

This result matches with the previous study which was conducted using neem chip biochar produced for the removal of mancozeb. They reported that the adsorption capacity (Qe in mg/g) increases with initial concentration (Manoharan et al., 2022). An increasing trend in the study of methyl orange dye removal using engineered biochar from neem chips was also reported (Sunthar et al., 2023).

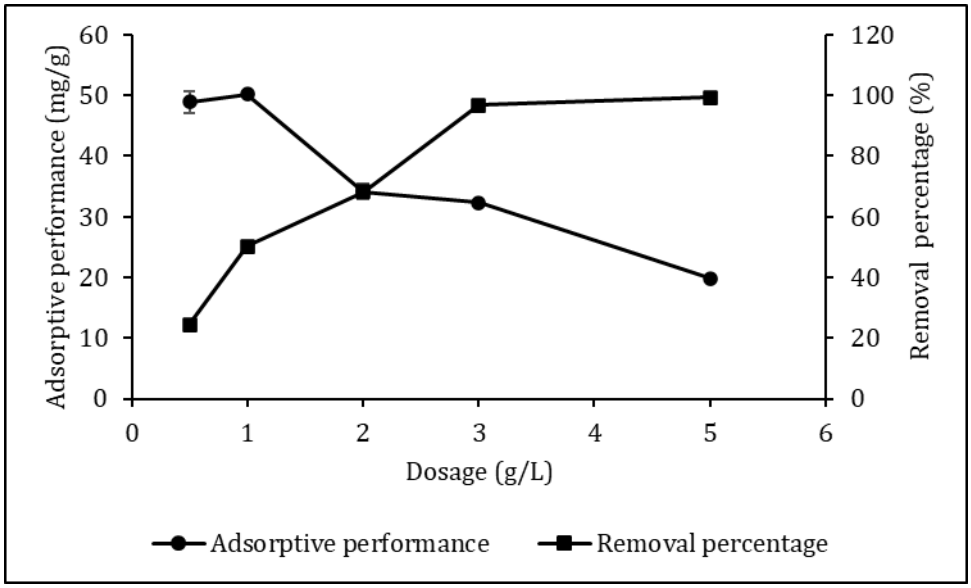

Figure 5. Effect of dosage on Malachite Green removal by engineered biochar

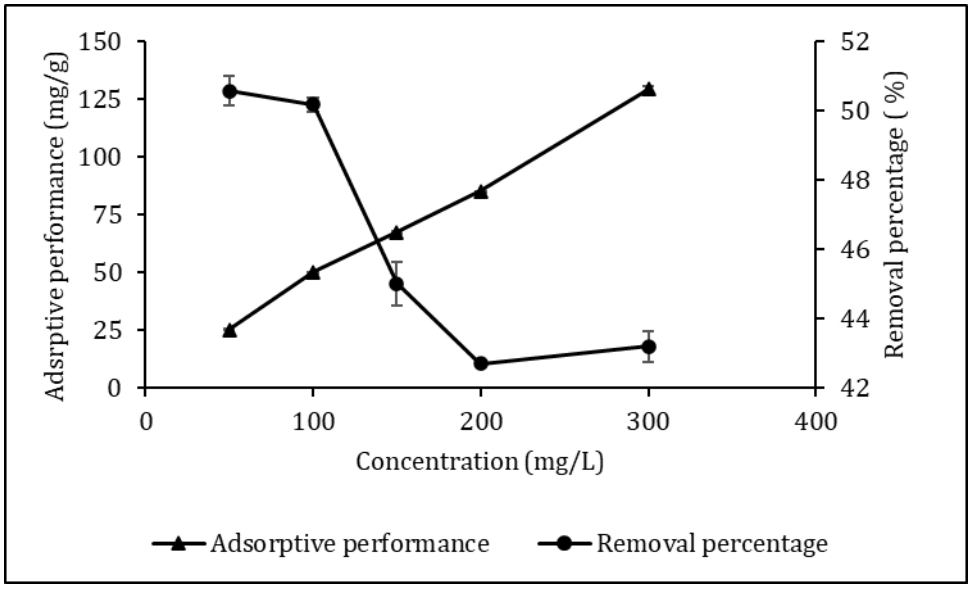

Figure 6. Effect of initial concentration on Malachite Green removal

pH

The effect of pH on the removal of Malachite Green by 9% CSBC 400 is illustrated in Figure 7. Higher adsorptive performance (Qe in mg/g) of Malachite Green was achieved at the pH of 6, whereas lower adsorptive performance was observed at the pH of 2. The pzc value of 9% CSBC 400 is 4.2(Figure 2). The pH plays a significant role in adsorptive performance. According to the previous study, the surface's acidic functional groups (such as carboxylic acid, phenolic, and alcohol) are accountable for adsorbing the malachite green dye. When the surface holds a negative charge, it attracts cationic dyes. At pH levels below the point of zero charge (pzc), the presence of H+ ions cause a repulsive effect against the cationic malachite green dye. However, when the pH exceeds the pzc, a negative surface charge develops, ultimately supporting the adsorption process.(Sangeetha piriya et al., 2021). Hence, At the pH below the value of 4.2(pzc), the surface of the biochar is positively charged to cause repulsion with Malachite Green molecules, and it reduces the removal of Malachite Green from the solution. When the pH of the solution approaches the value of 4.2 (pzc), the biochar is negatively charged and increases the interaction with Malachite Green molecules for better removal. The main factor governing adsorption is not surface area but pH(Sunthar et al., 2023). Also, the adsorption capacity is not solely linked to surface area; it is affected by both of the pH of the solution and the pzc of the biochar.(John et al., 2018; Sangeetha piriya et al., 2021)

Adsorption Isotherms

The sorption capacity, adsorption intensity, and heat of sorption for 9% CSBC 400 used for removing Malachite Green dye in water were assessed using three different models: Langmuir, Freundlich, and Temkin isotherm models. Linear forms of each model were used for the mathematical analysis. The findings from applying Langmuir, Freundlich, and Temkin models for fitting the outcomes of Malachite Green adsorption by 9% CSBC 400 are presented in Table 2. The Langmuir model represents an appropriate framework for monolayer adsorption, suggesting uniform adsorption energies across all sites on the adsorption surface. In contrast, the Freundlich model suits heterogeneous surfaces and continues to enhance its absorption capacity at higher concentrations. The Temkin model operates under the assumption that adsorption heat decreases linearly concerning the intensity of interaction between the adsorbate and adsorbent (Manoharan et al., 2022).

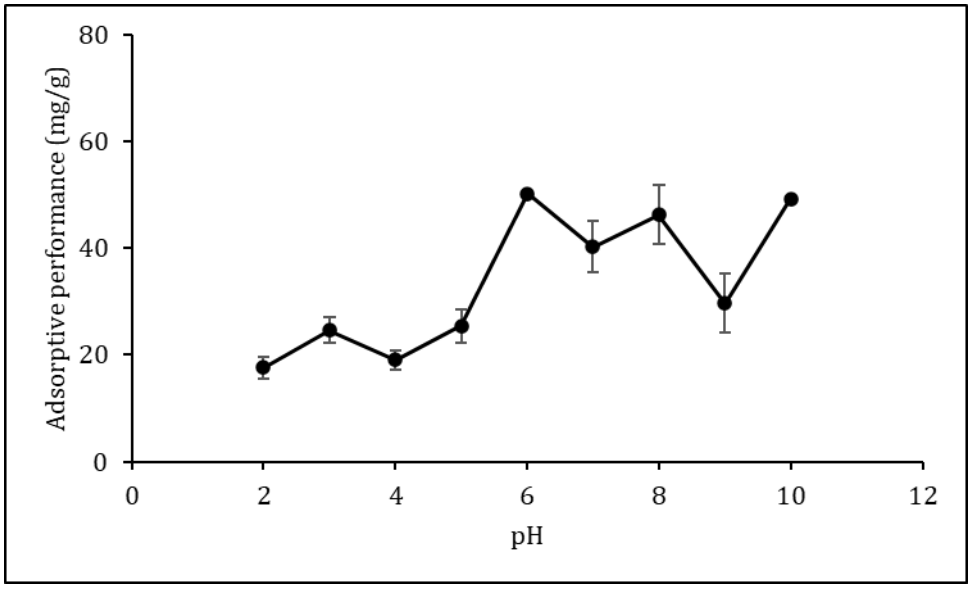

Figure 7. Effect of initial pH on Malachite Green removal (Temperature-27 ˚C; Dosage- 1 g/L; Initial concentration-100 mg/L)

Table 2. Parameters for Langmuir, Freundlich, and Temkin isotherm models Malachite Green adsorption to engineered biochar

Langmuir equation			Freundlich equation			Temkin equation		
R^2	Q_m	K_L	R^2	1/n	K_f	R^2	b_t	A_t
0.7834	368.66	0.0029	0.9908	0.8120	0.7656	0.9207	49.697	0.0576

Table 3. Kinetic parameters of Malachite Green Adsorption by 9% CSBC 400

Ci (mg/L)	Pseudo–first order				Pseudo-second order				Elovich		
	q_e. cal. (mg/g)	q_e. exp. (mg/g)	K_1	R^2	q_e. cal. (mg/g)	q_e. exp. (mg/g)	K_2	R^2	α	β	R^2
50	1209.41	25.76	0.0014	0.8693	26.24	25.76	0.00007	0.9488	0.2613	0.2523	0.8904
100	7917.64	44.49	0.0017	0.7673	44.73	44.49	0.00003	0.9461	0.6666	0.1811	0.9191
150	74.23	67.15	0.0005	0.9219	73.61	67.15	0.00001	0.9661	0.4975	0.1038	0.8784

Data linked to the Freundlich model display the most favorable overall regression coefficient and a better fit when compared to the other two models. The R^2 value from the Langmuir model is comparatively low, which suggests its non-applicability for the adsorption of Malachite Green dye(Hajialigol and Masoum, 2019). Consequently, the parameters from the Freundlich model were specifically considered to gain a deeper understanding of how the engineered biochar interacts with Malachite Green in adsorbing it. The R^2 value associated with the Freundlich model stands at 0.9908, while the coefficient of heterogeneity (1/n) for this model measures 0.8120. This value, falling between 0 and 1, signifies the favorability of the adsorption process (Manoharan et al., 2022). Considering this information, the adsorption of 9% CSBC 400 aligns well with the Freundlich isotherm model. Furthermore, this indicates that the adsorption of Malachite Green dye happens on heterogeneous surfaces in a multilayer mode (Nadarajah et al., 2021). Similarly, the adsorption of Methyl orange on the surface of neem chip-engineered biochar, and the adsorption of Malachite Green dye on coconut shell-derived $ZnCl_2$ activated carbon showed the Freundlich model as a best-suited model (Sangeetha piriya et al., 2021; Sunthar et al., 2023).

Adsorption Kinetics

The investigation involved studying the kinetics of Malachite Green under varying initial concentrations of 50, 100, and 150 mg/L. Three distinct kinetic models, Pseudo-first order, Pseudo-second order, and Elovich, were applied to elucidate the adsorption mechanism of Malachite Green by 9% CSBC 400. Table 3 presents the results derived from employing these models to analyze the adsorption of Malachite Green by 9% CSBC 400. It provides the R^2 values obtained from linear regression, along with additional parameters such as K_1 – adsorption rate constant for the pseudo-first order model, K_2-adsorption rate constant of the pseudo-second order model, α – initial adsorption rate, and β – desorption constant acquired from the corresponding graphs associated with each model. The pseudo-second order model yields R^2 values of 0.9482, 0.9461, and 0.9661 for 50, 100, and 150 mg /L concentrations, respectively.

The pseudo-second order model indicates a superior correlation compared to the pseudo-first order and Elovich models. Opting for the Pseudo-second order analysis enhances understanding by eliminating the impact of equilibrium concentration. However, due to the prolonged time needed for chemisorption

during adsorption to reach equilibrium, this model provides a less precise fit for the kinetic study despite its comprehensive insight into the adsorption process (Nadarajah et al., 2021). In this study, higher R^2 values indicate the significant role of equilibrium concentration in Malachite Green's removal rate, confirming chemisorption's impact during adsorption. Within the Pseudo-second order model, the calculated q_e (q_e. cal) closely resembles the experimental q_e (q_e. exp) values. Consequently, considering these observations, the Pseudo second-order model effectively delineates the kinetics of Malachite Green adsorption by 9% CSBC 400. It strongly suggests that chemisorption significantly influences the adsorption process, reinforcing the model's suitability in describing this phenomenon (Nadarajah et al., 2021).

Adsorption thermodynamics

An investigation into adsorption thermodynamics aimed to assess 9% CSBC 400's adsorptive performance under varying temperatures and determine the spontaneity and endothermic nature of the adsorption process. The investigation encompassed three temperature settings: 27 °C, 33 °C, and 37 °C. ΔH° and ΔS°, critical thermodynamic parameters, were deduced from the graph depicted in Figure 8, while Table 4 outlines the specific thermodynamic values related to Malachite Green adsorption. Evaluating Gibbs free energy (ΔG°) involves considering both enthalpy and entropy aspects, determining the spontaneity of adsorption, and the feasibility of the reaction. This comprehensive study indicates how temperature influences 9% CSBC 400's adsorptive capability and the energetic aspects governing the process.

When ΔG° values are negative, as observed at 27 °C (-18.7831 J/mol), 33 °C (-3.786kJ/mol), and 37 °C (-4.198 kJ/mol), it indicates the spontaneity of the Malachite Green adsorption onto coconut shell engineered biochar at these respective temperatures. This finding confirms the feasibility of the adsorption process across the temperature range (Vithanage et al., 2016). Additionally, the positive enthalpy change (ΔH°) of 130.8136 kJ/mol for Malachite Green indicates that the adsorption was of an endothermic nature. Hence, the removal efficiency of the Malachite Green can be increased by rising the temperature of the system up to a limit. Furthermore, the entropy change (ΔS°) of 0.4372 kJ/mol K offers insights into the binding or repulsive forces within the system. The positive ΔS° value (1.0066 kJ/mol K) implies an affinity of 9% CSBC 400 towards Malachite Green was strong, elucidating the structural alterations occurring within 9% CSBC 400 during the adsorption process (Nadarajah et al., 2021; Vithanage et al., 2016).Additionally, the positive value of ΔS° also suggests that the increasing randomness at the solid/liquid interface during the sorption of Malachite Green to the surface of the engineered biochar (Nadarajah et al., 2021).

Rate limiting analysis

Rate-limiting factor analysis, derived from kinetics study data. This study is crucial in comprehending how compounds traverse the surface and penetrate the pore spaces of biochar. This analysis is important to identify a more impactful rate-limiting process during the adsorption of Malachite Green. The Weber-Morris model was used to explore this limiting factor (Nadarajah et al., 2021). The linear plot of qt versus √t is demonstrated in Figure 9. Intraparticle diffusion (K_{wm}, mg/g. $min^{1/2}$) (inter-particle diffusion rate) and I (boundary layer thickness) were determined from the slope and intercept, respectively, across three initial concentration levels. Figure 10 depicts the relationship between K_{wm}/I and initial concentration.

The analysis of the Weber-Morris model revealed two different phases in the adsorption of Malachite green to the engineered biochar. In the qt versus √t plot, the first linear phase signifies the migration of Malachite Green from the solution to the biochar's surface. The subsequent linear phase represents Malachite Green's movement through the biochar's surface and internal pathways. Notably, the steeper slope in phase 1 for concentrations of 50, 100, and 150 mg/L indicates rapid Malachite Green particle movement to the biochar's outer surface. This accelerated movement is due to the compelling forces generated by surface functional groups of the engineered biochar

9% CSBC 400 (Sreedhar and Reddy, 2019). Consequently, the lower slopes of the second linear phase of the Weber-Morris analysis reveal the effect of intraparticle diffusion rate after a long reaction time (Nadarajah et al., 2021).

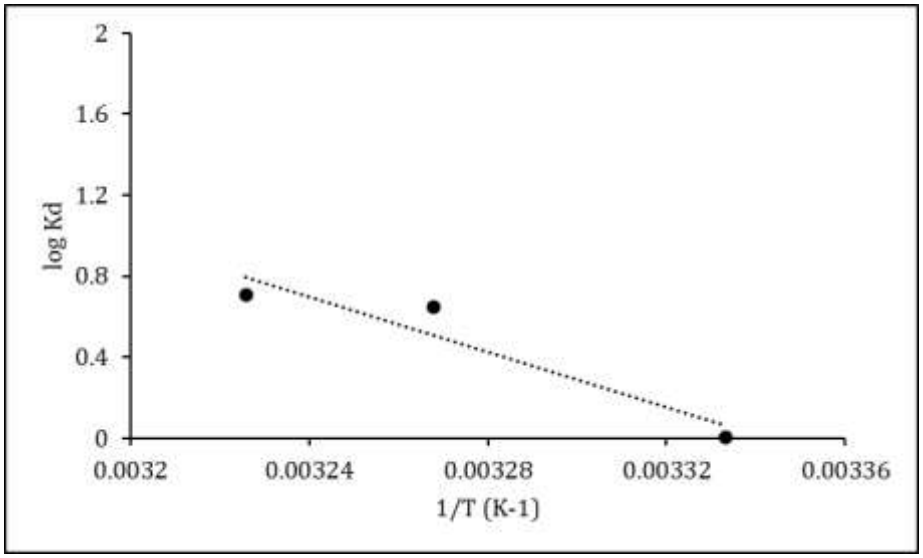

Figure 8. Relationship between log kd and 1/T

Table 2. Thermodynamic parameters of Malachite Green adsorption to 9% CSBC 400 adsorption

Dye	Temperature (K)	Thermodynamic parameters		
		ΔG°(KJ/mol)	ΔH°(KJ/mol)	ΔS° (KJ/mol K)
Malachite Green	300	-0.0188	130.8136	0.4372
	306	-3.7857		
	310	-4.1985		

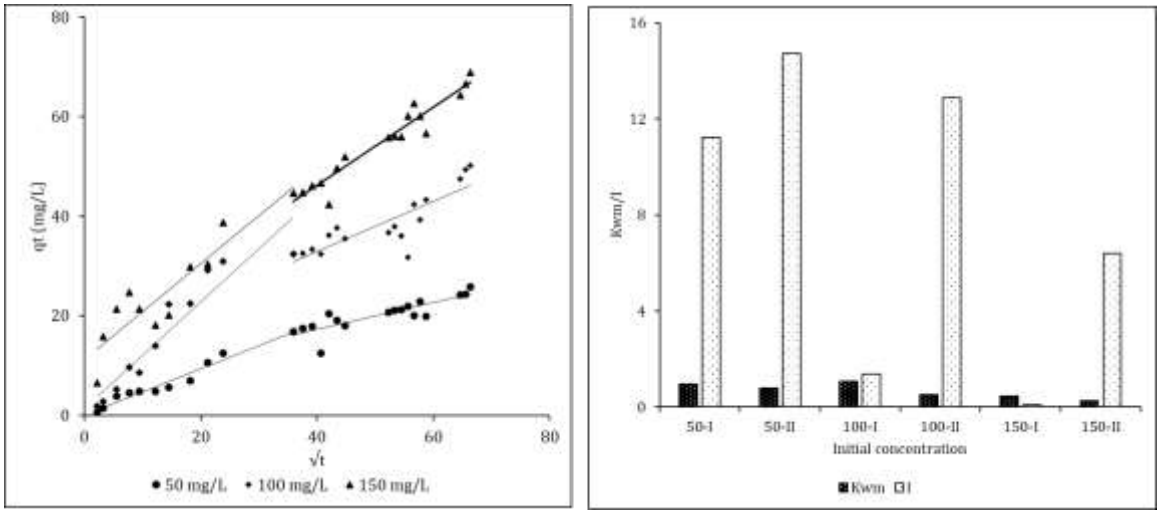

Figure 9. Rate limiting factor analysis of Malachite green adsorption by engineered biochar

According to reports, intercept value I > 1.0 indicates that both boundary layer thickness and intraparticle diffusion rate govern the rate-limiting impact (Kalavathy et al., 2005). Consequently, results for I from the second stage of the adsorption of Malachite Green at various concentrations point to the impact of both intraparticle diffusion and boundary layer on the overall removal efficiency (Nadarajah et al., 2021).

CONCLUSION

The scientific investigation into engineered biochar derived from coconut shells for removing Malachite Green produced promising results for cost-effective removal strategies compared to current sophisticated methods. The study indicates that coconut shells can be used to produce engineered adsorbents by activating them with $FeCl_3$ to remove Malachite Green from wastewater. The research suggests the potential for further modifications to achieve commercial-level performance. The biochar treated with 9% $FeCl_3$ and pyrolyzed at 400 °C showed the highest adsorption capacity of 50.20 mg/g for Malachite Green due to increased mineral components and a denser carbon network. Isotherm analysis revealed that the Freundlich model fits well, explaining the adsorption nature of Malachite Green by 9% CSBC 400 is multi-layer. The kinetic study showed that the pseudo-second order model fits well, indicating that the chemisorption process plays a significant role in the removal of Malachite Green by 9% CSBC 400. The adsorption process is spontaneous and endothermic, providing valuable information for determining the optimal temperature and conditions for removing Malachite Green from water.

REFERENCES

Abate, G.Y., Alene, A.N., Habte, A.T., Getahun, D.M., 2020. Adsorptive removal of malachite green dye from aqueous solution onto activated carbon of Catha edulis stem as a low cost bio-adsorbent. Environmental Systems Research 9, 29.

Ahmad, M., Rajapaksha, A.U., Lim, J.E., Zhang, M., Bolan, N., Mohan, D., Vithanage, M., Lee, S.S., Ok, Y.S., 2014. Biochar as a sorbent for contaminant management in soil and water: A review. Chemosphere 99, 19–33.

Alipour, M., Vosoughi, M., Mokhtari, S.A., Sadeghi, H., Rashtbari, Y., Shirmardi, M., Azad, R., 2021. Optimising the basic violet 16 adsorption from aqueous solutions by magnetic graphene oxide using the response surface model based on the Box–Behnken design. Int J Environ Anal Chem 101, 758–777.

Cha, J.S., Park, S.H., Jung, S.-C., Ryu, C., Jeon, J.-K., Shin, M.-C., Park, Y.-K., 2016. Production and utilization of biochar: A review. Journal of Industrial and Engineering Chemistry 40, 1–15.

Chatterjee, R., Sajjadi, B., Chen, W.-Y., Mattern, D.L., Hammer, N., Raman, V., Dorris, A., 2020. Effect of Pyrolysis Temperature on PhysicoChemical Properties and Acoustic-Based Amination of Biochar for Efficient CO2 Adsorption. Front Energy Res 8.

Dagnaw, L.A., Cherie, D.A., 2021. Point Zero Charge Determination and Fluoride Adsorption on Natural Red Ash (Metal Oxide). Asian Journal of Applied Chemistry Research 1–6.

Farooq, M., Ramli, A., 2011. The determination of point zero charge (PZC) of Al<inf>2</inf>O<inf>3</inf>-MgO mixed oxides. In: 2011 National Postgraduate Conference. IEEE, pp. 1–5.

Garg, V.K., Gupta, R., Bala Yadav, A., Kumar, R., 2003. Dye removal from aqueous solution by adsorption on treated sawdust. Bioresour Technol 89, 121–124.

Geetha, P., Latha, M.S., Koshy, M., 2015. Biosorption of malachite green dye from aqueous solution by calcium alginate nanoparticles: Equilibrium study. J Mol Liq 212, 723–730.

Hajialigol, S., Masoum, S., 2019. Optimization of biosorption potential of nano biomass derived from walnut shell for the removal of Malachite Green from liquids solution: Experimental design approaches. J Mol Liq 286, 110904.

Imran, M., Iqbal, M.M., Iqbal, J., Shah, N.S., Khan, Z.U.H., Murtaza, B., Amjad, M., Ali, S., Rizwan, M., 2021. Synthesis, characterization and application of novel MnO and CuO impregnated biochar composites to sequester arsenic (As) from

water: Modeling, thermodynamics and reusability. J Hazard Mater 401, 123338.

Jeganathan, Y., Asharp, T., Nadarajah, K., 2024. Adsorptive behavior of engineered biochar /hydrochar for tetracycline removal from synthetic wastewater. Environmental Pollution 345, 123452.

Jia, Y., Shi, S., Liu, J., Su, S., Liang, Q., Zeng, X., Li, T., 2018. Study of the Effect of Pyrolysis Temperature on the Cd2+ Adsorption Characteristics of Biochar. Applied Sciences 8, 1019.

John, Y., David, V.E., Mmereki, D., 2018. A Comparative Study on Removal of Hazardous Anions from Water by Adsorption: A Review. International Journal of Chemical Engineering 2018, 1–21.

Kalavathy, M.H., Karthikeyan, T., Rajgopal, S., Miranda, L.R., 2005. Kinetic and isotherm studies of Cu(II) adsorption onto H3PO4-activated rubber wood sawdust. J Colloid Interface Sci 292, 354–362.

Li, D.-C., Ding, J.-W., Qian, T.-T., Zhang, S., Jiang, H., 2016. Preparation of high adsorption performance and stable biochar granules by FeCl 3 -catalyzed fast pyrolysis. RSC Adv 6, 12226–12234.

Li, Y., Yang, T., Qi, X., Qiao, Y., Deng, A., 2008. Development of a group selective molecularly imprinted polymers based solid phase extraction of malachite green from fish water and fish feed samples. Anal Chim Acta 624, 317–325.

M. Idris, Z. Ahmad, M.A.A., 2011. Adsorption equilibrium of malachite green dye onto rubber seed coat based activated carbon.

Manoharan, T., Ganeshalingam, S., Nadarajah, K., 2022. Mechanisms of emerging contaminants removal by novel neem chip biochar. Environmental Advances 7, 100158.

Mittal, A., Mittal, J., Malviya, A., Gupta, V.K., 2009. Adsorptive removal of hazardous anionic dye "Congo red" from wastewater using waste materials and recovery by desorption. J Colloid Interface Sci 340, 16–26.

Modirshahla, N., Behnajady, M.A., 2006. Photooxidative degradation of Malachite Green (MG) by UV/H2O2: Influence of operational parameters and kinetic modeling. Dyes and Pigments 70, 54–59.

Moumeni, O., Hamdaoui, O., 2012. Intensification of sonochemical degradation of malachite green by bromide ions. Ultrason Sonochem 19, 404–409.

Nadarajah, K., Bandala, E.R., Zhang, Z., Mundree, S., Goonetilleke, A., 2021. Removal of heavy metals from water using engineered hydrochar: Kinetics and mechanistic approach. Journal of Water Process Engineering 40.

Oladoja, N.A., Aliu, Y.D., 2009. Snail shell as coagulant aid in the alum precipitation of malachite green from aqua system. J Hazard Mater 164, 1496–1502.

Oladoye, P.O., Ajiboye, T.O., Wanyonyi, W.C., Omotola, E.O., Oladipo, M.E., 2023. Insights into remediation technology for malachite green wastewater treatment. Water Science and Engineering 16, 261–270.

Pal, J., Deb, M.K., Deshmukh, D.K., Verma, D., 2013. Removal of methyl orange by activated carbon modified by silver nanoparticles. Appl Water Sci 3, 367–374.

Pan, X., Zhang, D., 2009. Removal of malachite green from water by Firmiana simplex wood fiber. Electronic Journal of Biotechnology 12.

Pandit, P., Basu, S., 2004. Removal of Ionic Dyes from Water by Solvent Extraction Using Reverse Micelles. Environ Sci Technol 38, 2435–2442.

Pirsaheb, M., Shahmoradi, B., Khosravi, T., Karimi, K., Zandsalimi, Y., 2016. Solar degradation of malachite green using nickel-doped TiO_2 nanocatalysts. Desalination Water Treat 57, 9881–9888.

Raval, A.R., Kohli, H.P., Mahadwad, O.K., 2022. Application of emulsion liquid membrane for removal of malachite green dye from aqueous solution: Extraction and stability studies. Chemical Engineering Journal Advances 12, 100398.

Raval, N.P., Shah, P.U., Shah, N.K., 2017a. Malachite green "a cationic dye" and its removal from aqueous solution by adsorption. Appl Water Sci 7, 3407–3445.

Raval, N.P., Shah, P.U., Shah, N.K., 2017b. Malachite green "a cationic dye" and its removal from aqueous solution by adsorption. Appl Water Sci 7, 3407–3445.

Ronsse, F., van Hecke, S., Dickinson, D., Prins, W., 2013. Production and characterization of slow pyrolysis biochar: Influence of

feedstock type and pyrolysis conditions. GCB Bioenergy 5, 104–115.

Saha, S., Wang, J.M., Pal, A., 2012. Nano silver impregnation on commercial TiO2 and a comparative photocatalytic account to degrade malachite green. Sep Purif Technol 89, 147–159.

Sangeetha piriya, R., Jayabalakrishnan, R.M., Maheswari, M., Boomiraj, K., Oumabady, S., 2021. Coconut shell derived ZnCl2 activated carbon for malachite green dye removal. Water Science and Technology 83, 1167–1182.

Santhi, T., Manonmani, S., 2011. Malachite Green Removal from Aqueous Solution by the Peel of Cucumis sativa Fruit. Clean (Weinh) 39, 162–170.

Sharma, J., Sharma, S., Soni, V., 2023. Toxicity of malachite green on plants and its phytoremediation: A review. Reg Stud Mar Sci 62, 102911.

Sreedhar, I., Reddy, N.S., 2019. Heavy metal removal from industrial effluent using bio-sorbent blends. SN Appl Sci 1, 1021.

Sunthar, L., Asharp, T., Nadarajah, K., 2023. Insights into Mechanisms of Novel Engineered Biochar Derived from Neem Chips via Iron Catalyst for the Removal of Methyl Orange from Aqueous Phase. Water Air Soil Pollut 234, 178.

Tewari, K., Singhal, G., Arya, R.K., 2018. Adsorption removal of malachite green dye from aqueous solution. Reviews in Chemical Engineering 34, 427–453.

Tomczyk, A., Sokołowska, Z., Boguta, P., 2020. Biochar physicochemical properties: pyrolysis temperature and feedstock kind effects. Rev Environ Sci Biotechnol 19, 191–215.

Vithanage, M., Mayakaduwa, S.S., Herath, I., Ok, Y.S., Mohan, D., 2016. Kinetics, thermodynamics and mechanistic studies of carbofuran removal using biochars from tea waste and rice husks. Chemosphere 150, 781–789.

Zhou, X.-J., Guo, W.-Q., Yang, S.-S., Zheng, H.-S., Ren, N.-Q., 2013. Ultrasonic-assisted ozone oxidation process of triphenylmethane dye degradation: Evidence for the promotion effects of ultrasonic on malachite green decolorization and degradation mechanism. Bioresour Technol 128, 827–830.